



Exclusive and diffractive $\gamma\gamma$ production in $PbPb$ collisions at the LHC, HE-LHC and FCC

R. O. Coelho^{1,a}, V. P. Gonçalves^{1,b}, D. E. Martins^{2,c}, M. Rangel^{2,d}

¹ Instituto de Física e Matemática, Universidade Federal de Pelotas (UFPEl), Caixa Postal 354, Pelotas, RS CEP 96010-090, Brazil

² Instituto de Física, Universidade Federal do Rio de Janeiro (UFRJ), Caixa Postal 68528, Rio de Janeiro, RJ CEP 21941-972, Brazil

Received: 2 March 2020 / Accepted: 2 May 2020 / Published online: 30 May 2020

© The Author(s) 2020

Abstract In this paper we present a detailed analysis of the contribution of the Light-by-Light (LbL), Durham and double diffractive processes for the diphoton production in ultraperipheral $PbPb$ collisions at the Large Hadron Collider (LHC), High-Energy LHC (HE-LHC) and Future Circular Collider (FCC). The acceptance of the central and forward LHC detectors is taken into account and predictions for the invariant mass, rapidity, transverse momentum and acoplanarity distributions are presented. Our results indicate that the contribution of the Durham process is negligible and that the double diffractive process can be strongly suppressed by the exclusivity cuts, which will allow to perform a precise analysis of the LbL scattering, as well the search of beyond Standard Model physics in this final state.

1 Introduction

Light-by-light (LbL) scattering is a very rare phenomenon in which two photons interact, producing another pair of photons. This process was one of the most important predictions in the beginning of Quantum Electrodynamics (QED), and has no parallel in classical electrodynamics theory. Direct evidence for light-by-light scattering at high energy had proven difficult to detect for decades. Although LbL scattering via an electron loop has been indirectly tested through the high precision measurements of the electron and muon anomalous magnetic moment [1,2], direct observations in the laboratory remained inconclusive until recently, when the CMS and ATLAS Collaboration have observed, for the first time, the light-by-light (LbL) scattering in ultraperipheral PbPb Collisions [3,4]. Such collisions are characterized

by an impact parameter b greater than the sum of the radius of the colliding nuclei [5–13] and by a photon–photon luminosity that scales with Z^4 , where Z is number of protons in the nucleus. As a consequence, in ultraperipheral heavy ion collisions (UPHIC), the elementary elastic $\gamma\gamma \rightarrow \gamma\gamma$ process, which occurs at one-loop level at order α^4 and have a tiny cross section, is enhanced by a large Z^4 ($\approx 45 \times 10^6$) factor, becoming it feasible for the experimental analysis [14,15]. The LbL scattering in ultraperipheral $PbPb$ collisions is represented in Fig. 1a, with the resulting final state being very clean, consisting of the diphoton system, two intact nuclei and two rapidity gaps, i.e. empty regions in pseudo-rapidity that separate the intact very forward nuclei from the $\gamma\gamma$ system. The recent experimental results have motivated a series of studies that propose the analysis of the diphoton production in $\gamma\gamma$ interactions as a probe of Beyond Standard Model (BSM) physics (See e.g. Refs. [16–19]). However, in order to be possible to search by New Physics in $\gamma\gamma$ channel, it is fundamental to have control of background associated to other production channels that also generated a similar final state. Two potential backgrounds are the diphoton production in central exclusive processes induced by gluons, represented in Fig. 1b and denoted Durham process hereafter, and in double diffractive processes, represented in Fig. 1c, d. Such reactions also are characterized by two rapidity gaps and two intact ions in the final state, but the diphoton system is generated by the interaction between gluons of the nucleus (Durham process) or gluons of the Pomeron (\mathbb{P}), which is a color singlet object inside the nucleus, in the case of double diffractive processes. One of goals of this paper is to estimate the contribution of each one of these production channels taking into account the acceptance of the LHC detectors, presenting for the first time the predictions associated to the double diffractive process. In particular, we will consider the typical set of cuts used by the ATLAS and CMS Collaborations to separate the exclusive events. In addition, we will present, for the first time, a detailed comparison between these distinct channels for the

^a e-mail: coelho72@gmail.com

^b e-mail: barros@ufpel.edu.br (corresponding author)

^c e-mail: dan.ernani@gmail.com

^d e-mail: rangel@if.ufjf.br

diphoton production in the kinematical range probed by the LHCb detector (For a previous study of the LbL scattering at the LHCb see Ref. [20]). We will explore the possibility present in this detector of probe diphotons with small invariant mass. A second goal of our paper is to present predictions for the diphoton production in $PbPb$ collisions for the energies of the High-Energy LHC ($\sqrt{s} = 10.6$ TeV) [21] and Future Circular Collider ($\sqrt{s} = 39$ TeV) [22] (See also Ref. [23,24]). In order to obtain the results for these future colliders we will consider the typical configurations of central and forward detectors and similar cuts to those used to LHC. As we will demonstrate below, the possibility of probe the LbL scattering in the LHCb detector is very promising, as well at the HE-LHC and FCC. Our results indicate that the background associated to the Durham process is negligible and that the contribution of the double diffractive processes can be strongly suppressed, which will allow to perform a detailed study of the LbL scattering as well the search of BSM physics using this final state.

This paper is organized as follows. In the next section, we present a brief review of the formalism used to describe the diphoton production in $PbPb$ collisions by the LbL, Durham and double diffractive processes. Moreover, we discuss the treatment of the soft survival effects. In Sect. 3, we present our results for the $\gamma\gamma$ production at the LHC, HE-LHC and FCC. Predictions for cross sections and the invariant mass, rapidity, transverse momentum and acoplanarity distributions are presented. The impact of the selection cuts is discussed and predictions for a typical central and forward detector are presented. Finally, in Sect. 4, our main conclusions are summarized.

2 Formalism

Initially, we present a brief review of the main formulas to describe the exclusive diphoton production by $\gamma\gamma$ interactions in ultraperipheral $PbPb$ collisions, represented in Fig. 1a. Assuming the impact parameter representation and considering the Equivalent Photon Approximation (EPA) [25], the total cross section can be factorized in terms of the equivalent photon spectrum of the incident nuclei and the elementary cross section for the elastic $\gamma\gamma \rightarrow \gamma\gamma$ process as follows

$$\begin{aligned} \sigma(PbPb \rightarrow Pb \otimes \gamma\gamma \otimes Pb; s) \\ = \int d^2\mathbf{r}_1 d^2\mathbf{r}_2 dW dY \frac{W}{2} \hat{\sigma}(\gamma\gamma \rightarrow \gamma\gamma; W) \\ \times N(\omega_1, \mathbf{r}_1) N(\omega_2, \mathbf{r}_2) S_{abs}^2(\mathbf{b}). \end{aligned} \quad (1)$$

where \sqrt{s} is center-of-mass energy of the $PbPb$ collision, \otimes characterizes a rapidity gap in the final state, $W = \sqrt{4\omega_1\omega_2} = m_X$ is the invariant mass of the $\gamma\gamma$ system and

$Y = y_{\gamma\gamma}$ its rapidity. The photon energies ω_1 and ω_2 are related to W and to the rapidity Y of the outgoing diphoton system by

$$\omega_1 = \frac{W}{2} e^Y \quad \text{and} \quad \omega_2 = \frac{W}{2} e^{-Y}. \quad (2)$$

The cross section $\hat{\sigma}$ is the elementary cross section to produce a pair of photons, which will be calculated taking into account of the fermion loop contributions as well as the contribution from W bosons. Moreover, $N(\omega_i, \mathbf{r}_i)$ is the equivalent photon spectrum with energy ω_i at a transverse distance \mathbf{r}_i from the center of nucleus, defined in the plane transverse to the trajectory, which is determined by the charge form factor of the nucleus. Finally, the factor $S_{abs}^2(\mathbf{b})$ depends on the impact parameter \mathbf{b} of the $PbPb$ collision and is denoted the absorptive factor, which excludes the overlap between the colliding nuclei and allows to take into account only ultraperipheral collisions. Currently, there are different approaches to treat these soft survival corrections. For example, Baur and Ferreira-Filho [27] have proposed to exclude the strong interactions between the incident nuclei by assuming that

$$S_{abs}^2(\mathbf{b}) = \Theta(|\mathbf{b}| - 2R) = \Theta(|\mathbf{b}_1 - \mathbf{b}_2| - 2R), \quad (3)$$

where R is the nuclear radius. Such equation treats the nuclei as hard spheres with radius R and assumes that the probability to have a hadronic interaction when $b > 2R$ is zero. On the other hand, in the STARLight [28] and SuperChic [29] event generators, the authors have proposed distinct models based on the Glauber formalism. We have verified that for small values of W , which is the focus of the analysis performed in this paper, the predictions of these different approaches are almost identical, in agreement with the analysis performed in Ref. [26] where the authors have presented a detailed analysis about the description of exclusive $\gamma\gamma$ interactions in $PbPb$ collisions considering different models for the form factor and for the absorptive corrections. In our calculations we express Eq. (1) in the momentum space in order to impose cuts that depend on the photon transverse momenta.

For the exclusive production of a diphoton in the gluon-induced interactions represented in Fig. 1b, we will consider the model proposed by Khoze, Martin and Ryskin [30–32] some years ago, denoted Durham model hereafter, which has been used to estimate a large number of different final states and have predictions in reasonable agreement with the observed rates for exclusive processes measured by the CDF collaboration [33–35] and in the Run I of the LHC (For a recent review see Ref. [36]). In this model, the amplitude for the diphoton production in a pp collision can be expressed as follows

$$\begin{aligned} \mathcal{A}_{pp}(s, q_{1\perp}, q_{2\perp}) \\ = \pi^2 \int \frac{d^2Q_{\perp} \bar{\mathcal{M}}}{Q_{\perp}^2 q_{1\perp}^2 q_{2\perp}^2} f_g(x_1, x'_1, Q_{\perp}^2, \mu^2; t_1) \end{aligned}$$

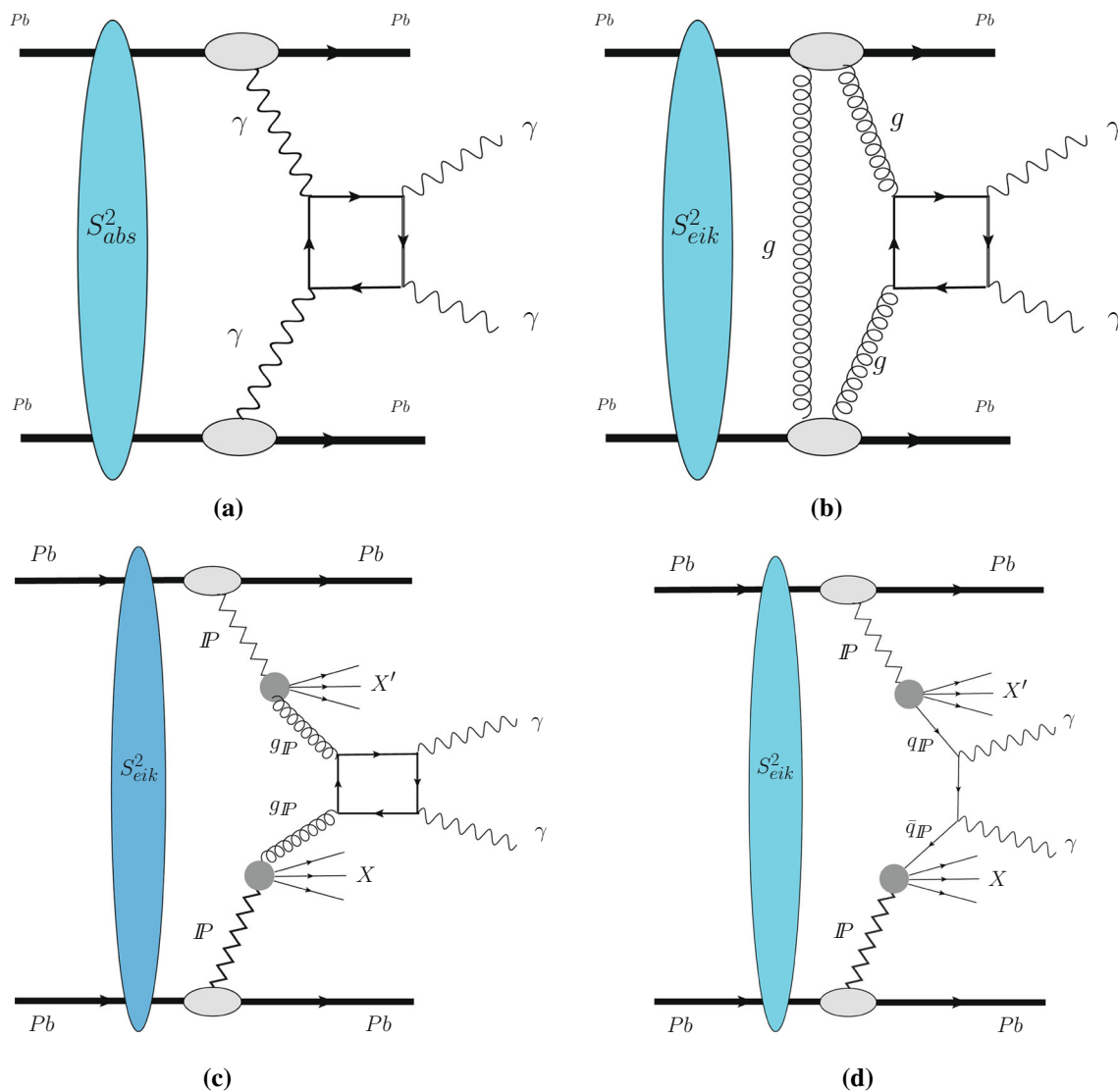


Fig. 1 Diphoton production in $PbPb$ collisions by **a** the Light-by-Light scattering, **b** the central exclusive process induced by gluons (Durham process), and the double diffractive processes induced by **c** gluons and **d** quarks of the Pomeron (\mathbb{P})

$$\times f_g(x_2, x'_2, Q_{\perp}^2, \mu^2; t_2) \tag{4}$$

where Q_{\perp}^2 is the virtuality of the soft gluon needed for color screening, $q_{1\perp}$ and $q_{2\perp}$ are the transverse momenta of the gluons which participate of the hard subprocess and x_i (x'_i) are the momentum fractions carried by the fusing (screening) gluons. Moreover, $\bar{\mathcal{M}}$ is the color-averaged, normalized sub-amplitude for the $gg \rightarrow \gamma\gamma$ subprocess. The quantities f_g are the skewed unintegrated gluon densities evaluated to the factorization scale μ , which we assume to be of the order of the invariant mass m_X of the final state. The t -dependence of the skewed distribution is assumed to factorize out as a proton form factor, being $\propto \exp(bt/2)$ with $b = 4 \text{ GeV}^{-2}$. Since

$$\left(x' \approx \frac{Q_{\perp}}{\sqrt{s}}\right) \ll \left(x \approx \frac{m_X}{\sqrt{s}}\right) \ll 1 \tag{5}$$

it is possible to express $f_g(x, x', Q_{\perp}^2, \mu^2)$, to single log accuracy, in terms of the conventional integrated gluon density $g(x)$, together with a known Sudakov suppression T which ensures that the active gluons do not radiate in the evolution from Q_{\perp} up to the hard scale $\mu \approx m_X/2$. In this paper we will calculate f_g in the proton case considering that the integrated gluon distribution xg is described by the MMHT parametrization [37]. The Eq. (4) corresponds to the amplitude for the exclusive production of a diphoton in a hard process without no further perturbative emission. However, the exclusivity of the event can be spoiled by secondary particles that can be produced by additional soft hadronic interactions. Such soft survival effects are, in general, parametrized in terms of a rapidity gap survival probability, S^2 , which corresponds to the probability of the scattered proton not

to dissociate due to the secondary interactions. In Ref. [29] the Durham model was generalized for ion–ion collisions by proposing to express the scattering amplitude for the coherent $A_1 A_2$ process in terms of the pp amplitude described above and the nuclear form factors F_{A_i} as follows

$$\mathcal{A}_{A_1 A_2}(s, q_{1\perp}, q_{2\perp}) = \mathcal{A}_{pp}(s, q_{1\perp}, q_{2\perp}) F_{A_1}(Q_1^2) F_{A_2}(Q_2^2), \quad (6)$$

where $Q_i^2 = (q_{i\perp}^2 + x_i^2 m_{N_i}^2)/(1 - x_i)$. Such equation was written in the impact parameter space and a model for the soft survival effects was included in the calculation. The resulting ion–ion cross section is proportional to the pp one and to the nuclear opacity, which encodes the probability for no additional ion–ion rescattering at different impact parameters. One important aspect is that the nuclear version of the Durham model is implemented in the SuperChic3 Monte Carlo event generator, being possible to perform the analysis with and without the inclusion of the soft survival effects. In our analysis we will consider the fully exclusive diphoton production, denoted coherent ion–ion QCD-induced central exclusive process (CEP) in Ref. [29]. However, the diphoton can also be produced in incoherent QCD-induced processes, where the individual nucleons remain intact due to the diffractive nature of the interaction, but the ions break up. As shown in Ref. [29], the cross section for these semi-exclusive processes is larger than for the coherent one by a factor ≈ 2 . If the ion dissociation is not seen by the detector, the coherent and incoherent processes contribute for the exclusive diphoton rate.

Finally, for the description of the diphoton production in the double diffractive processes (DDP) represented in Fig. 1c, d, we will consider the Resolved Pomeron model, in which the pomeron is assumed to have a partonic structure [38]. We have that the corresponding cross section can be expressed by

$$\begin{aligned} \sigma(PbPb \rightarrow Pb \otimes X + \gamma\gamma + X' \otimes Pb) \\ = \left\{ \int dx_1 \int dx_2 \left[g_1^D(x_1, \mu^2) \cdot g_2^D(x_2, \mu^2) \cdot \hat{\sigma}(gg \rightarrow \gamma\gamma) \right. \right. \\ \left. \left. + [q_1^D(x_1, \mu^2) \cdot \bar{q}_2^D(x_2, \mu^2) \right. \right. \\ \left. \left. + \bar{q}_1^D(x_1, \mu^2) \cdot q_2^D(x_2, \mu^2)] \cdot \hat{\sigma}(q\bar{q} \rightarrow \gamma\gamma) \right] \right\}, \quad (7) \end{aligned}$$

where $g_i^D(x_i, \mu^2)$, $q_i^D(x_i, \mu^2)$ and $\bar{q}_i^D(x_i, \mu^2)$ are the diffractive gluon, quark and antiquark densities of the nucleus i with a momentum fraction x_i . In the Resolved Pomeron model [38] the diffractive parton distributions are expressed in terms of parton distributions in the pomeron and a Regge parametrization of the flux factor describing the pomeron emission by the hadron. The parton distributions have its evolution given by the DGLAP evolution equations and should be determined from events with a rapidity gap or a intact hadron. In order to specify the diffractive distributions for a

nucleus, we will follow the approach proposed in Ref. [39] (See also Ref. [40]). In this approach, the diffractive distributions for a nucleus are estimated taking into account the nuclear effects associated to the nuclear coherence and the leading twist nuclear shadowing. The basic assumption is that the pomeron–nucleus coupling is proportional to the mass number A [42]. As the associated pomeron flux depends on the square of this coupling, this model predicts that the pomerons are coherently emitted by the nucleus, which implies that the pomeron flux emitted by the nucleus, $f_{\mathbb{P}/A}$, is proportional to A^2 . Consequently, the nuclear diffractive gluon distribution can be expressed as follows (For details see Ref. [39])

$$g_A^D(x, \mu^2) = R_g A^2 \int_x^1 \frac{dx_{\mathbb{P}}}{x_{\mathbb{P}}} \left[\int dt f_{\mathbb{P}/p}(x_{\mathbb{P}}, t) \cdot F_A^2(t) \right] \times g_{\mathbb{P}}\left(\frac{x}{x_{\mathbb{P}}}, \mu^2\right), \quad (8)$$

where R_g is the suppression factor associated to the nuclear shadowing, $f_{\mathbb{P}/p}(x_{\mathbb{P}}, t)$ is the pomeron flux emitted by the proton and $g_{\mathbb{P}}(\beta, \mu^2)$ is the gluon distribution in the pomeron, with β being the momentum fraction carried by the partons inside the pomeron. Moreover, $F_A(t)$ is the nuclear form factor. A similar relation is also valid for the diffractive quark and antiquark densities of the nucleus. In what follows we will assume that $R_g = 0.15$ as in Ref. [39] and that $F_A(t) \propto e^{R_A^2 t/6}$, with R_A being the nuclear radius. It is important to emphasize that our group have implemented this generalization in the Forward Physics Monte Carlo (FPMC) [41], which allow us to estimate the associated cross sections and distributions taking into account of the detector acceptances. The hard matrix elements are treated by interfacing FPMC with HERWIG v6.5 which includes perturbative parton showering followed by the hadronization. In double diffractive events, the pomeron remnants are generated with a similar strategy as the proton remnants in proton–proton collisions, hence they are expected to be soft and to populate the forward and backward directions. Experimentally, part of the energy carried out by pomeron remnants is not detected due to either a limited rapidity coverage of the calorimeter or due to a minimum energy readout threshold in the system. However, the presence of remnants can give a significant boost to the diphotons in the transverse plane resulting in a non-negligible azimuthal decorrelation between them. Finally, in double diffractive processes, the rapidity gap is smaller than in the exclusive diphoton case due to the presence of pomeron remnants which partially occupy the gap due to pomeron exchange.

Similarly to the exclusive case, the predictions for the diphoton production in double diffractive processes are also expected to be strongly modified by soft interactions which lead to an extra production of particles that destroy the rapid-

ity gaps in the final state [43]. As these effects have non-perturbative nature, they are difficult to treat and its magnitude is strongly model dependent (For recent reviews see Refs. [44,45]). In our analysis of the soft survival corrections in ion-ion collisions we will assume that they can be factorized of the hard process and that its effects can be included in the calculation by multiplying the cross section by a global factor S_{eik}^2 (denoted eikonal factor). Such assumption is based on the idea that the hard process occurs on a short enough timescale such that the physics that generate the additional particles can be factorized and accounted by an overall factor. The validity of this assumption for double diffractive processes in nuclear collisions is still an open question and should be considered a first approximation for this difficult problem. In our analysis we will estimate S_{eik}^2 considering the approach proposed in Ref. [46], which generalizes the model described in Ref. [42] for coherent double exchange processes in nuclear collisions. The basic idea in this approach is to express the double diffractive cross section in the impact parameter space, which implies that it becomes dependent on the magnitude of the geometrical overlap of the two nuclei during the collision. As a consequence, it is possible to take into account the centrality of the incident particles and estimate the absorptive corrections associated to the additional soft hadronic interactions by requiring that the colliding nuclei remain intact, which is equivalent to suppress the interactions at small impact parameters ($b < R_A + R_B$). A detailed description of this approach is presented in Appendix A of Ref. [46]. The resulting predictions for $PbPb$ collisions at $\sqrt{s} = 5.5, 10.6$ and 39 TeV are $3.4 \times 10^{-5}, 2.1 \times 10^{-5}$ and 1.0×10^{-5} , respectively. It is important to emphasize that these predictions are larger than those obtained in Ref. [47] using a Glauber approach and in Ref. [48] assuming that the nuclear suppression factor is given by $S_{A_1 A_2}^2 = S_{pp}^2 / (A_1 \cdot A_2)$. For the exclusive diphoton process represented by the Fig. 1b, we will include the soft survival effects using the model proposed in Ref. [29], which is implemented in the SuperChic MC. As will show below, this model implies a larger impact of these effects on the exclusive cross sections than the model developed in Ref. [46] for double diffractive processes. In our calculations we will estimate the exclusive diphoton using the SuperChic MC and its own model for S_{eik}^2 , while the double diffractive process will be calculated using the FPMC and its predictions will be multiplied by the factor S_{eik}^2 derived in Ref. [46].

3 Results

In what follows we will present our results for the exclusive and diffractive diphoton production in $PbPb$ collisions at $\sqrt{s} = 5.5, 10.6$ and 39 TeV. In our analysis we will use the SuperChic MC event generator [29] to estimate the processes

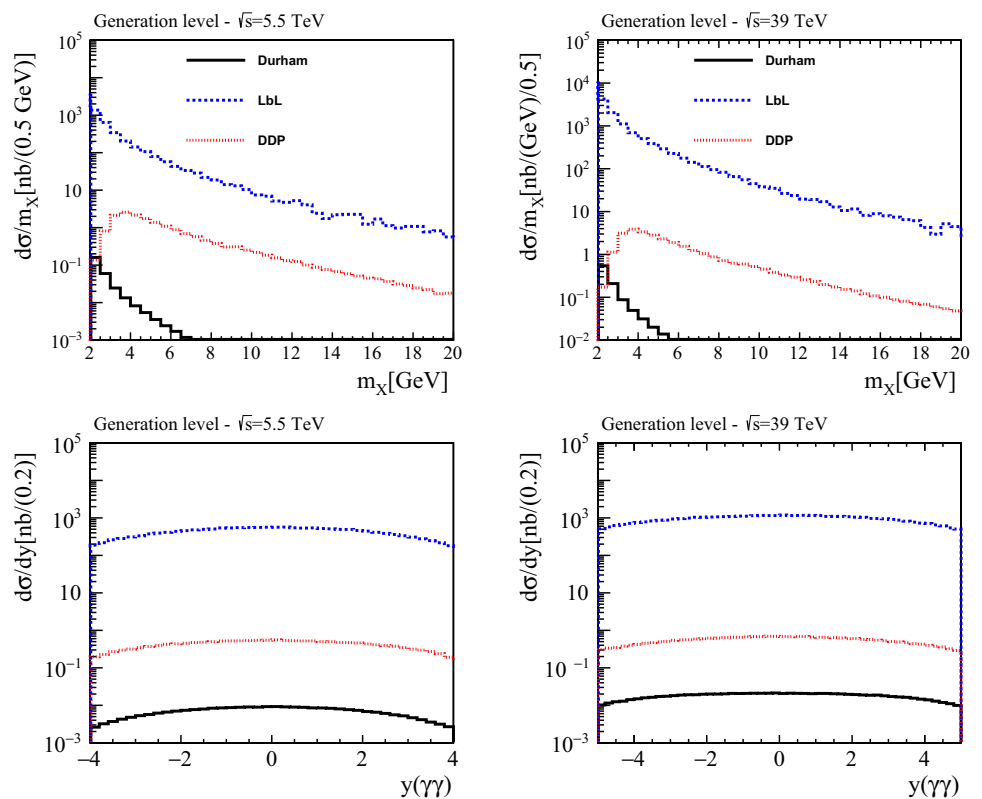
Table 1 Predictions for the diphoton production cross sections in $PbPb$ collisions at LHC, HE-LHC and FCC. The results in the parenthesis are the predictions after the inclusion of soft survival factor S_{eik}^2

Process	\sqrt{s} (TeV)	$\sigma[Pb Pb \rightarrow Pb + \gamma\gamma + Pb]$
LbL	5.5	1.8×10^4 nb
	10.6	2.7×10^4 nb
	39	5.2×10^4 nb
Durham	5.5	4.9×10^6 nb (0.280 nb)
	10.6	9.8×10^6 nb (0.570 nb)
	39	3.8×10^7 nb (0.980 nb)
DDP	5.5	5.2×10^5 nb (17.7 nb)
	10.6	9.7×10^5 nb (22.3 nb)
	39	3.0×10^6 nb (30.0 nb)

represented in the Fig. 1a, b. On the other hand, the double diffractive diphoton production (Fig. 1c, d), will be calculated considering the FPMC event generator [41]. Initially, in Table 1 we present our results for the cross sections associated to the different channels, obtained at the generation level, without the inclusion of any selection in the events. We have that the gluon-induced processes (Durham and DDP) are strongly suppressed by the soft survival effects, with the associated cross sections being a factor $\geq 10^3$ smaller than the photon-induced one (LbL). Moreover, without the inclusion of the survival corrections, the Durham prediction is one order of magnitude larger than the DDP one. When these corrections are taken into account, the DDP predictions become two orders of magnitude larger than the Durham one, which demonstrates the large impact of the soft survival effects in the exclusive channel. In Fig. 2 we present our results for the invariant mass (m_X) and the rapidity ($y_{\gamma\gamma}$) distributions of the diphoton system for $PbPb$ collisions at the LHC (left panels) and FCC (right panels). One has that the LbL dominates the diphoton production in the m_X and $y_{\gamma\gamma}$ ranges considered. In addition, our results indicate that the double diffractive prediction is larger than the Durham one for $m_X > 3$ GeV, but are similar at small invariant mass.

In order to obtain realistic estimates of the diphoton production in $PbPb$ collisions, which can be compared with the future experimental data, we will include in our analysis the experimental cuts that are expected to be feasible in the next run of the LHC and in the future at the HE-LHC and FCC. We will consider two distinct configurations of cuts: one for a typical central detector as ATLAS and CMS, and other for a forward detector as LHCb. In particular, we will analyze the possibility of study diphotons with invariant mass in the range $1 \leq m_X \leq 5$ GeV using the LHCb detector. Currently, such low mass range cannot be reached by the central detectors. The selection criteria implemented in our analysis of

Fig. 2 Predictions for the invariant mass m_X and rapidity $y_{\gamma\gamma}$ distributions of the diphoton system produced in $PbPb$ collisions at the LHC (left panels) and FCC (right panels). Results at the generation level, without the inclusion of experimental cuts



double diffractive and exclusive diphoton processes are the following:

- For a central detector: We will select events in which $m_X > 5$ GeV and $E_T(\gamma, \gamma) > 2$ GeV, where E_T is the transverse energy of the photons. Moreover, we will impose a cut on the acoplanarity ($1 - (\Delta\phi/\pi) < 0.01$) and transverse momentum of the diphoton system ($p_T(\gamma, \gamma) < 0.1$ GeV). Finally, we only will select events where photons are produced in the rapidity range $|\eta(\gamma^1, \gamma^2)| < 2.5$ with 0 extra tracks.
- For a forward detector: We will select events in which $m_X > 1$ GeV and $p_T(\gamma, \gamma) > 0.2$ GeV, where p_T is the transverse momentum of the photons. Moreover, we will impose a cut on the acoplanarity ($1 - (\Delta\phi/\pi) < 0.01$) and transverse momentum of the diphoton system ($p_T(\gamma, \gamma) < 0.1$ GeV). Finally, we only will select events where photons are produced in the rapidity range $2.0 < |\eta(\gamma^1, \gamma^2)| < 4.5$ with 0 extra tracks with $p_T > 0.1$ GeV in the rapidity range $-3.5 < \eta < -1.5$ and $p_T > 0.5$ GeV in the range $-8.0 < \eta < -5.5$.

The impact of each of these cuts in the different processes for the LHC, HE-LHC and FCC energies is presented in the Tables 2 and 3 for a central and forward detector, respectively. For the central detector configuration, we have that the cut in the invariant mass has a large impact in the LbL and Durham processes. Such impact is smaller in the case of a forward

detector, since the events with small invariant masses are included. The LbL and Durham predictions are not strongly modified by the inclusion of the other cuts, unless of the cut on rapidity for a forward detector which suppress the cross section by one order of magnitude. In addition, our results indicate that the inclusion of all cuts fully suppress the contribution of the double diffractive process for the diphoton production. In particular, we have that this contribution is completely removed by the cut on the transverse momentum of the diphoton system ($p_T(\gamma\gamma) < 0.1$ GeV), before to apply the exclusivity cut on extra tracks which are expected to be present due to the Pomeron remnants. The impact of the transverse momentum cut is associated to the fact that in the double diffractive production the transverse momentum of the gluons inside the Pomeron, which interact to generate the diphoton, can be large. In contrast, in the exclusive production, we have that the typical transverse momentum of the diphoton is determined by the transferred momentum in the Pomeron–nucleus vertex. As the exclusive cross section has an $e^{-\beta|t|}$ behavior, where β is the slope parameter associated, the associated p_T distribution decreases exponentially at large transverse momentum. Therefore, it is expected that the production of a diphoton with a large p_T should be dominated by the diffractive mechanism. On the other hand, if only events with $p_T \leq 0.1$ GeV are selected, the observed diphoton system will be mainly produced by the exclusive process. Finally, we predict that the contribution of the Durham model for the exclusive $\gamma\gamma$ production is five orders of magnitude

Table 2 Predictions for the central exclusive and double diffractive diphoton cross sections after the inclusion of the exclusivity cuts for a typical central detector

	LbL	Durham	DDP
<i>PbPb</i> collisions at $\sqrt{s} = 5.5$ TeV			
Total cross section [nb]	18000.0	0.28	17.7
$m_X > 5$ GeV, $E_T(\gamma, \gamma) > 2$ GeV	187.0	0.006	17.7
$1 - (\Delta\phi/\pi) < 0.01$	186.0	0.005	6.9
$p_T(\gamma\gamma) < 0.1$ GeV	139.0	0.005	0.1
$ \eta(\gamma, \gamma) < 2.5$ and 0 extra tracks	139.0	0.003	0.0
<i>PbPb</i> collisions at $\sqrt{s} = 10.6$ TeV			
Total cross section [nb]	27000.0	0.57	22.3
$m_X > 5$ GeV, $E_T(\gamma, \gamma) > 2$ GeV	352.9	0.01	13.5
$1 - (\Delta\phi/\pi) < 0.01$	352.8	0.01	0.1
$p_T(\gamma\gamma) < 0.1$ GeV	350.2	0.01	0.0
$ \eta(\gamma, \gamma) < 2.5$ and 0 extra tracks	227.6	0.006	0.0
<i>PbPb</i> collisions at $\sqrt{s} = 39$ TeV			
Total cross section [nb]	52000.0	0.98	30.0
$m_X > 5$ GeV, $E_T(\gamma, \gamma) > 2$ GeV	844.0	0.02	13.0
$1 - (\Delta\phi/\pi) < 0.01$	840.0	0.02	0.1
$p_T(\gamma\gamma) < 0.1$ GeV	836.0	0.02	0.0
$ \eta(\gamma, \gamma) < 2.5$ and 0 extra tracks	431.0	0.009	0.0

Table 3 Predictions for the central exclusive and double diffractive diphoton cross sections after the inclusion of the exclusivity cuts for a typical forward detector

	LbL	Durham	DDP
<i>PbPb</i> collisions at $\sqrt{s} = 5.5$ TeV			
Total cross section [nb]	18000.0	0.28	17.7
$m_X > 1$ GeV, $p_T(\gamma, \gamma) > 0.2$ GeV	13559.0	0.24	17.6
$1 - (\Delta\phi/\pi) < 0.01$	8834.0	0.09	0.2
$p_T(\gamma\gamma) < 0.1$ GeV	8826.0	0.08	0.0
$2.0 < \eta(\gamma, \gamma) < 4.5$ and 0 extra tracks	616.0	0.006	0.0
<i>PbPb</i> collisions at $\sqrt{s} = 10.6$ TeV			
Total cross section [nb]	27000.0	0.57	22.3
$m_X > 1$ GeV, $p_T(\gamma, \gamma) > 0.2$ GeV	20372.9	0.49	22.0
$1 - (\Delta\phi/\pi) < 0.01$	13958.5	0.2	0.3
$p_T(\gamma\gamma) < 0.1$ GeV	13949.0	0.2	0.0
$2.0 < \eta(\gamma, \gamma) < 4.5$ and 0 extra tracks	1069.5	0.01	0.0
<i>PbPb</i> collisions at $\sqrt{s} = 39$ TeV			
Total cross section [nb]	52000.0	0.980	30.0
$m_X > 1$ GeV, $p_T(\gamma, \gamma) > 0.2$ GeV	38025.0	0.85	30.0
$1 - (\Delta\phi/\pi) < 0.01$	28216.0	0.3	0.3
$p_T(\gamma\gamma) < 0.1$ GeV	28202.0	0.3	0.0
$2.0 < \eta(\gamma, \gamma) < 4.5$ and 0 extra tracks	2229.0	0.03	0.0

smaller than the LbL process. Such result implies that the LbL process could be studied in the future run of the LHC, as well in the future HE-LHC and FCC, in a clean environment and reduced background, which will allow a detailed search by Beyond Standard Model physics using this final state.

In Fig. 3 we present our predictions for the invariant mass m_X , transverse momentum $p_T(\gamma\gamma)$, rapidity $y(\gamma\gamma)$ and acoplanarity distributions considering a central detector

Fig. 3 Results for the invariant mass m_X , transverse momentum $p_T(\gamma\gamma)$, rapidity $y(\gamma\gamma)$ and acoplanarity distributions considering a central detector and $PbPb$ collisions at the LHC (left panels) and FCC (right panels)

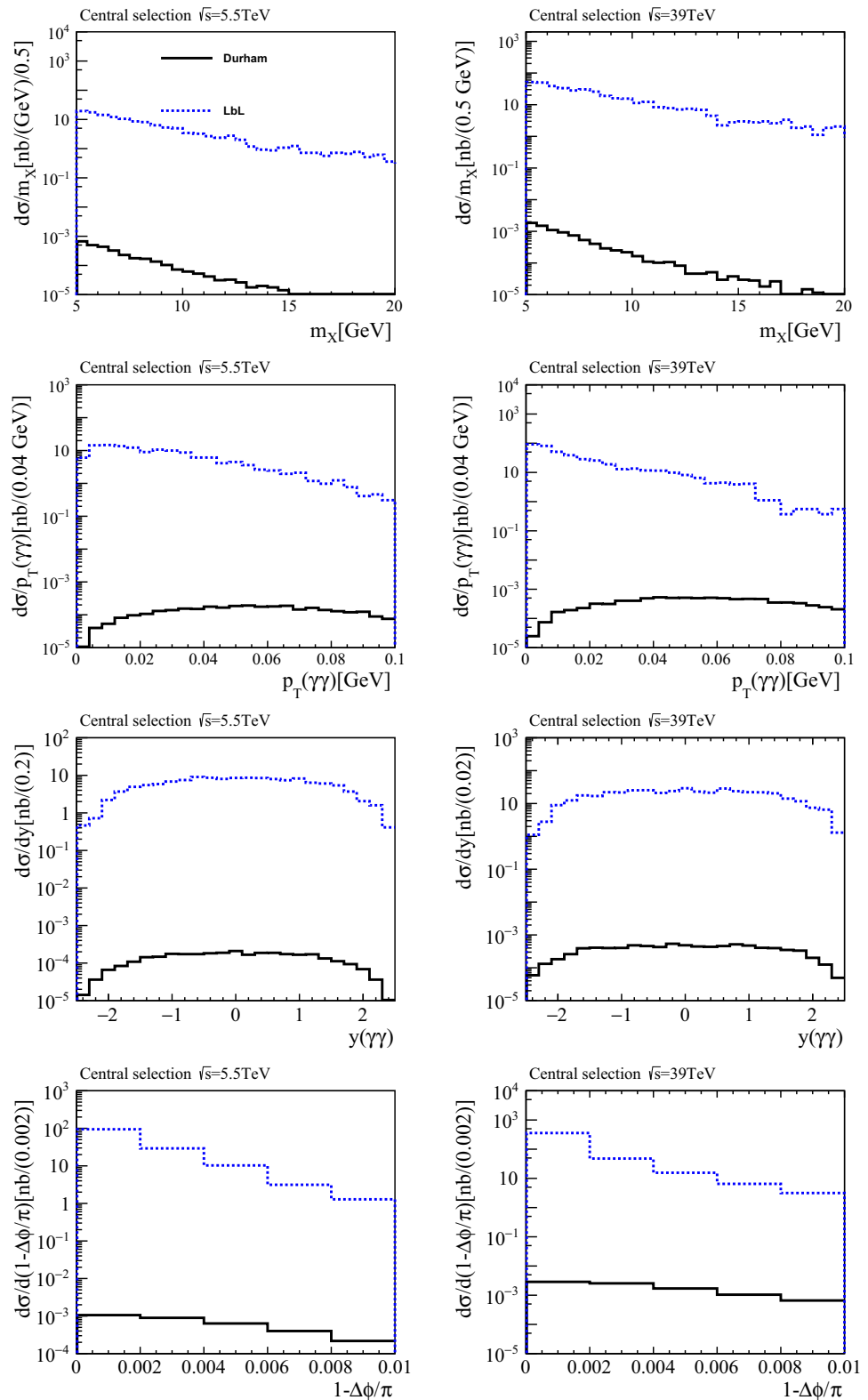
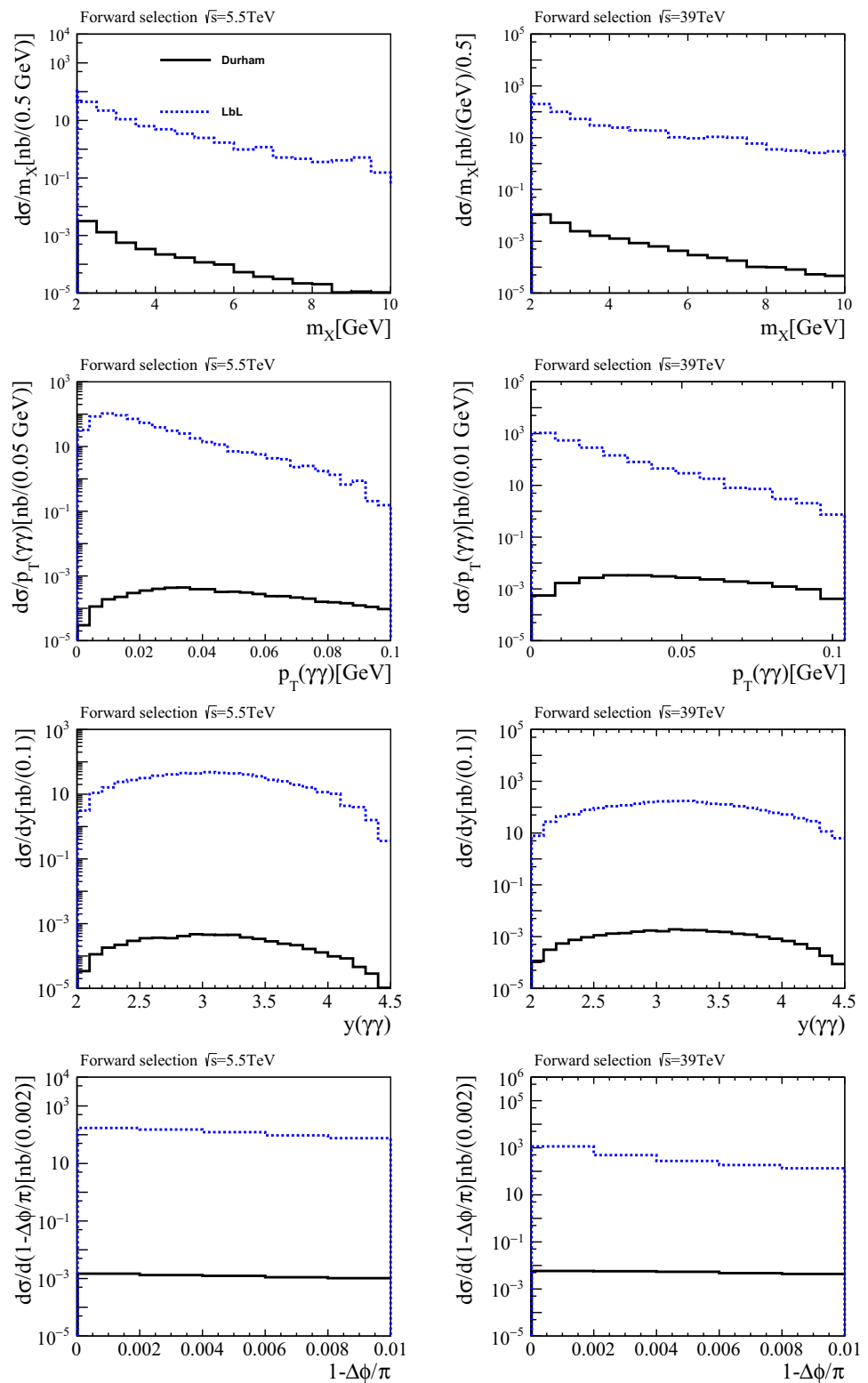


Fig. 4 Results for the invariant mass m_X , transverse momentum $p_T(\gamma\gamma)$, rapidity $y(\gamma\gamma)$ and acoplanarity distributions considering a forward detector and $PbPb$ collisions at the LHC (left panels) and FCC (right panels)



and $PbPb$ collisions at the LHC (left panels) and FCC (right panels). We have that the Durham process only becomes *non-negligible* for a diphoton system with a large transverse momentum. Similar results, but with a distinct normalization, are obtained for a forward detector, as verified in Fig. 4.

4 Summary

The high photon–photon luminosity present in ultraperipheral heavy-ion collisions become feasible the experimental analysis of different final state that can be used to test some of the more important properties of Standard Model (SM) as well to search by BSM physics. One of more interesting final states is the diphoton system, which can be produced by photon- and gluon-induced interactions. Although the elementary $\gamma\gamma \rightarrow \gamma\gamma$ and $gg \rightarrow \gamma\gamma$ subprocesses have a very tiny cross section, the associated $PbPb$ cross sections become measurable due to the large number of photons and gluons in the initial state. In this paper we have estimated the contribution of the Light-by-Light scattering, Durham and, for the first time, of the double diffractive processes for the diphoton production. The typical cuts used to select exclusive events were taken into account as well as the acceptance of the LHC detectors. In particular, a detailed analysis of the diphoton production in the kinematical range probed by the LHCb detector was performed by the first time. Moreover, we have presented predictions for the diphoton production in $PbPb$ collisions for the energies of the future High Energy-LHC and FCC. Our results demonstrated that the contribution of the gluon induced processes is small and that the double diffractive process can be strongly suppressed by the exclusivity cuts. Consequently, future experimental analysis of the diphoton production will allow to perform a precise study of the LbL process as well to search by New Physics using this final state.

Acknowledgements VPG acknowledge very useful discussions about photon-induced interactions with Gustavo Gil da Silveira, Mariola Klusek-Gawenda and Antoni Szczurek. This work was partially financed by the Brazilian funding agencies CNPq, CAPES, FAPERGS, FAPERJ and INCT-FNA (processes number 464898/2014-5 and 88887.461636/2019-00).

Data Availability Statement This manuscript has no associated data or the data will not be deposited. [Authors' comment: This is a theoretical research work and no additional data is associated.]

Open Access This article is licensed under a Creative Commons Attribution 4.0 International License, which permits use, sharing, adaptation, distribution and reproduction in any medium or format, as long as you give appropriate credit to the original author(s) and the source, provide a link to the Creative Commons licence, and indicate if changes were made. The images or other third party material in this article are included in the article's Creative Commons licence, unless indicated otherwise in a credit line to the material. If material is not included in the article's Creative Commons licence and your intended

use is not permitted by statutory regulation or exceeds the permitted use, you will need to obtain permission directly from the copyright holder. To view a copy of this licence, visit <http://creativecommons.org/licenses/by/4.0/>.
Funded by SCOAP³.

References

1. R.S. Van Dyck, P.B. Schwinberg, H.G. Dehmelt, Phys. Rev. Lett. **59**, 26 (1987)
2. Muon g-2 Collaboration, Phys. Rev. Lett. **86**, 2227 (2001)
3. G. Aad et al. [ATLAS Collaboration], Phys. Rev. Lett. **123**(5), 052001 (2019)
4. A.M. Sirunyan et al. [CMS Collaboration], Phys. Lett. B **797**, 134826 (2019)
5. C.A. Bertulani, G. Baur, Phys. Rep. **163**, 299 (1988)
6. F. Krauss, M. Greiner, G. Soff, Prog. Part. Nucl. Phys. **39**, 503 (1997)
7. G. Baur, K. Hencken, D. Trautmann, J. Phys. G **24**, 1657 (1998)
8. G. Baur, K. Hencken, D. Trautmann, S. Sadovsky, Y. Kharlov, Phys. Rep. **364**, 359 (2002)
9. C.A. Bertulani, S.R. Klein, J. Nystrand, Annu. Rev. Nucl. Part. Sci. **55**, 271 (2005)
10. V.P. Goncalves, M.V.T. Machado, J. Phys. G **32**, 295 (2006)
11. A.J. Baltz et al., Phys. Rep. **458**, 1 (2008)
12. J.G. Contreras, J.D. Tapia Takaki, Int. J. Mod. Phys. A **30**, 1542012 (2015)
13. K. Akiba et al. [LHC Forward Physics Working Group], J. Phys. G **43**, 110201 (2016)
14. D. d'Enterria, G.G. da Silveira, Phys. Rev. Lett. **111**, 080405 (2013) [Erratum: Phys. Rev. Lett. **116**(12), 129901 (2016)]
15. M. Klusek-Gawenda, P. Lebedowicz, A. Szczurek, Phys. Rev. C **93**(4), 044907 (2016)
16. S. Knapen, T. Lin, H.K. Lou, T. Melia, Phys. Rev. Lett. **118**(17), 171801 (2017)
17. C. Baldenegro, S. Hassani, C. Royon, L. Schoeffel, Phys. Lett. B **795**, 339 (2019)
18. Y.M.P. Gomes, J.T. Guaitolini Junior, Phys. Rev. D **99**(5), 055006 (2019)
19. L. Beresford, J. Liu, [arXiv:1908.05180](https://arxiv.org/abs/1908.05180) [hep-ph]
20. M. Klusek-Gawenda, R. McNulty, R. Schicker, A. Szczurek, Phys. Rev. D **99**(9), 093013 (2019)
21. A. Abada et al. [FCC Collaboration], Eur. Phys. J. ST **228**(5), 1109 (2019)
22. A. Abada et al. [FCC Collaboration], Eur. Phys. J. ST **228**(4), 755 (2019)
23. D. d'Enterria, G.G. da Silveira, [arXiv:1602.08088](https://arxiv.org/abs/1602.08088) [hep-ph]
24. A. Dainese et al., CERN Yellow Rep., no. 3, 635 (2017)
25. V.M. Budnev, I.F. Ginzburg, G.V. Meledin, V.G. Serbo, Phys. Rep. **15**, 181 (1975)
26. C. Azevedo, V.P. Goncalves, B.D. Moreira, Eur. Phys. J. C **79**(5), 432 (2019)
27. G. Baur, L.G. Ferreira Filho, Nucl. Phys. A **518**, 786 (1990)
28. S.R. Klein, J. Nystrand, J. Seger, Y. Gorbunov, J. Butterworth, Comput. Phys. Commun. **212**, 258 (2017)
29. L.A. Harland-Lang, V.A. Khoze, M.G. Ryskin, Eur. Phys. J. C **79**(1), 39 (2019)
30. V.A. Khoze, A.D. Martin, M.G. Ryskin, Eur. Phys. J. C **14**, 525 (2000)
31. V.A. Khoze, A.D. Martin, M.G. Ryskin, Eur. Phys. J. C **23**, 311 (2002)
32. V.A. Khoze, A.D. Martin, M.G. Ryskin, Eur. Phys. J. C **19**, 477 (2001) [Erratum-ibid. C **20**, 599 (2001)]

33. T. Aaltonen et al. [CDF Collaboration], *Phys. Rev. Lett.* **99**, 242002 (2007)
34. T. Aaltonen et al. [CDF Collaboration], *Phys. Rev. D* **77**, 052004 (2008)
35. T. Aaltonen et al. [CDF Collaboration], *Phys. Rev. Lett.* **102**, 242001 (2009)
36. L.A. Harland-Lang, V.A. Khoze, M.G. Ryskin, W.J. Stirling, *Int. J. Mod. Phys. A* **29**, 1430031 (2014)
37. L.A. Harland-Lang, A.D. Martin, P. Motylinski, R.S. Thorne, *Eur. Phys. J. C* **75**(5), 204 (2015)
38. G. Ingelman, P.E. Schlein, *Phys. Lett. B* **152**, 256 (1985)
39. V. Guzey, M. Klasen, *JHEP* **1604**, 158 (2016)
40. L. Frankfurt, V. Guzey, M. Strikman, *Phys. Rep.* **512**, 255 (2012)
41. M. Boonekamp, A. Dechambre, V. Juranek, O. Kepka, M. Rangel, C. Royon, R. Staszewski, [arXiv:1102.2531](https://arxiv.org/abs/1102.2531) [hep-ph]
42. B. Muller, A.J. Schramm, *Nucl. Phys. A* **523**, 677 (1991)
43. J.D. Bjorken, *Phys. Rev. D* **47**, 101 (1993)
44. V.A. Khoze, A.D. Martin, M.G. Ryskin, *Int. J. Mod. Phys. A* **30**(08), 1542004 (2015)
45. E. Gotsman, E. Levin, U. Maor, *Int. J. Mod. Phys. A* **30**(08), 1542005 (2015)
46. E. Basso, V.P. Goncalves, A.K. Kohara, M.S. Rangel, *Eur. Phys. J. C* **77**, 600 (2017)
47. E. Levin, J. Miller, [arXiv:0801.3593](https://arxiv.org/abs/0801.3593) [hep-ph]
48. V.P. Goncalves, W.K. Sauter, *Phys. Rev. D* **82**, 056009 (2010)